Femtosecond Nonlinear Fiber Optics in the Ionization Regime

P. Hölzer,[1] W. Chang,[1] J. C. Travers,[1] A. Nazarkin,[1] J. Nold,[1] N. Y. Joly,[2,1] M. F. Saleh,[1] F. Biancalana,[1] and P. St. J. Russell[1,2]

[1]*Max Planck Institute for the Science of Light, Günther-Scharowsky-Strasse 1, 91058 Erlangen, Germany*
[2]*Department of Physics, University of Erlangen-Nuremberg, 91054 Erlangen, Germany*

(Received 27 June 2011; published 7 November 2011)

By using a gas-filled kagome-style photonic crystal fiber, nonlinear fiber optics is studied in the regime of optically induced ionization. The fiber offers low anomalous dispersion over a broad bandwidth and low loss. Sequences of blueshifted pulses are emitted when 65 fs, few-microjoule pulses, corresponding to high-order solitons, are launched into the fiber and undergo self-compression. The experimental results are confirmed by numerical simulations which suggest that free-electron densities of $\sim 10^{17}$ cm^{-3} are achieved at peak intensities of 10^{14} W/cm^2 over length scales of several centimeters.

DOI: 10.1103/PhysRevLett.107.203901 PACS numbers: 42.65.Re, 32.80.Fb, 42.65.Ky, 42.81.Dp

Over the past few decades, the study of optically induced ionization in bulk gases or gas-filled capillaries has enabled the generation of attosecond pulses and extreme wavelengths via high harmonic generation [1–3]. Simultaneously, nonlinear fiber optics has progressed from the first demonstrations of solitons in glass fibers [4] to the generation of bright and coherent multioctave spanning supercontinua [5]. The root of the recent success in the latter case has been the versatile control of group velocity dispersion provided by photonic crystal fibers [6], especially in combination with soliton-driven dynamics. Here we report on the demonstration of soliton-driven ionization effects in gas-filled photonic crystal fibers—allowing the use of high-field plasma-based processes to complement the rich dynamics of nonlinear fiber optics. This combination represents a new regime in nonlinear optics, which could not be accessed by either of the two original systems alone.

Consisting of a kagome-style hollow core photonic crystal fiber (PCF) [6] filled with argon gas, our system offers broadband transmission at low loss (~ 1 dB/m) with a tight mode confinement and low anomalous dispersion (a few fs^2/cm) that can be balanced against the weak normal dispersion of the gas. This means, for example, that the zero-dispersion wavelength can be tuned from the UV to the IR simply by varying the gas pressure. This combination of properties has permitted high efficiency generation of tunable UV resonant radiation from femtosecond pulses at near-infrared wavelengths [7]. Here, in contrast, we tune the zero-dispersion wavelength deep into the UV (380 nm), far from the pump wavelength, so that perturbations caused by the emission of resonant radiation are negligible [8]. This allows us to explore ultrashort pulse propagation above the ionization threshold of the gas, thus combining soliton dynamics with plasma effects. (A companion Letter discusses a novel phenomenon in this system: the soliton self-frequency blueshift [9].) Higher-order solitons, launched into the fiber, undergo smooth temporal compression to the few-cycle regime through the combined effects of self-phase-modulation and anomalous dispersion in the absence of Raman scattering [10]. As a result, a pulse launched with a peak intensity well below the ionization threshold can be temporally focused to reach intensities of $\sim 10^{14}$ W/cm^2—sufficient to ionize the gas and create a plasma. For the first time it is possible to maintain well-controlled single-mode pulse propagation over several centimeters at ionization fractions approaching 1% (free-electron densities of $\sim 10^{17}$ cm^{-3}) at the few-microjoule level in the core of an optical fiber. These free-electron densities can exceed those usually observed in filamentation experiments in bulk gases, where the ionization fraction is constrained by the need to achieve nonlinear self-channeling [11].

Gas-filled hollow capillaries have been commonly used to spectrally broaden femtosecond pulses before externally compressing them down to the few-cycle regime [12] for the generation of high harmonics in either a gas jet or a second gas-filled capillary [1–3]. To avoid unacceptably high transmission losses, the inner diameter of the capillary needs to be ~ 200 μm, which in turn requires pulse energies of some 10–100 s of microjoule range if the ionization threshold is to be reached. Critically, such diameters prevent the easy adjustment of anomalous dispersion (which remains normal at useful gas pressures), which not only prevents the use of pulse self-compression but also means that they are unsuitable for studying the combined soliton-plasma effects reported in this Letter.

Recently, short ~ 1 cm lengths of kagome PCF have been used for low threshold high harmonic generation [13]; however, the gas pressures used were too low to access the soliton-plasma regime discussed here. An alternative fiber choice is a hollow core photonic band-gap-based PCF, but, despite the observation of weak plasma effects in such fibers [14], the narrow transmission windows, along with much higher values of group velocity

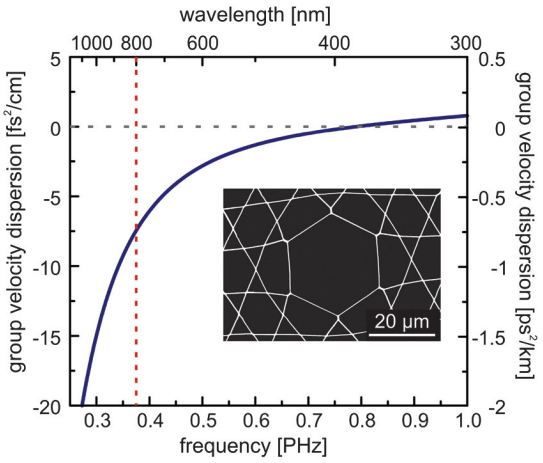

FIG. 1 (color). Calculated group velocity dispersion of a kagome-lattice PCF filled with 1.7 bar of Ar. The vertical dashed line denotes the pump frequency. The inset shows a scanning electron micrograph of the fiber core region.

dispersion with strong third-order terms, make them unsuitable for studies of soliton-plasma interactions [6,14].

In the experiments reported here, the kagome PCF had an effective core diameter of 26 μm and a transmission window from 600 to 1000 nm at a loss level of $\sim$2 dB/m. Its group velocity dispersion β_2, calculated by following the approach described in Ref. [15], is plotted in Fig. 1 for an Ar pressure of 1.7 bar and provides anomalous dispersion $|\beta_2| < 20$ fs^2/cm over the whole transmission window. Raman scattering is absent since a noble gas is used and the light-glass overlap is less than 1% [7]. Both ends of a 34 cm length of the fiber were fitted into gas cells. The fiber was then flushed with Ar, evacuated to remove any residual air, and filled with Ar to the required pressure. Pulses from a Ti:sapphire laser at 800 nm (energies up to 9 μJ, duration 65 fs) could be launched into the fiber without any noticeable damage, either optically induced or plasma-related. The output mode appeared to be fundamental for all energies.

Figure 2(a) shows experimental output spectra measured as a function of input pulse energy (soliton order $N = 11$ at $\sim$9 μJ). For pulse energies up to $\sim$1.5 μJ [region (i) in Fig. 2(a)], the spectrum broadens dramatically due to self-phase-modulation. A further increase in pulse energy results in visible light emitted through the side of the fiber, indicating the extreme pulse compression (and spectral expansion). First observable at the output end of the fiber, the emission moves back toward the fiber input with increasing pulse energy; i.e., as expected, the point of maximum temporal compression is reached more quickly at higher pulse energies. At these energies an extra peak, corresponding to a blueshifted pulse, appears on the blue side of the spectrum. This pulse is first visible at 750 nm for a pump energy of 2 μJ ($N \sim 5$), shifting to below 600 nm with increasing energy [region (ii) in Fig. 2(a)]. At even higher energies ($\sim$ 4 μJ), instead of further shifting, a second blueshifted pulse appears in the experimental spectrum. Clear spectral interference fringes can be observed between the two blueshifted pulses. Note that the spectral blueshift of each pulse saturates at higher pulse energies. Figure 2(d) shows that deviations from linear transmission can be seen, coinciding with the emission of the blueshifted sidebands and providing evidence of ionization-related losses.

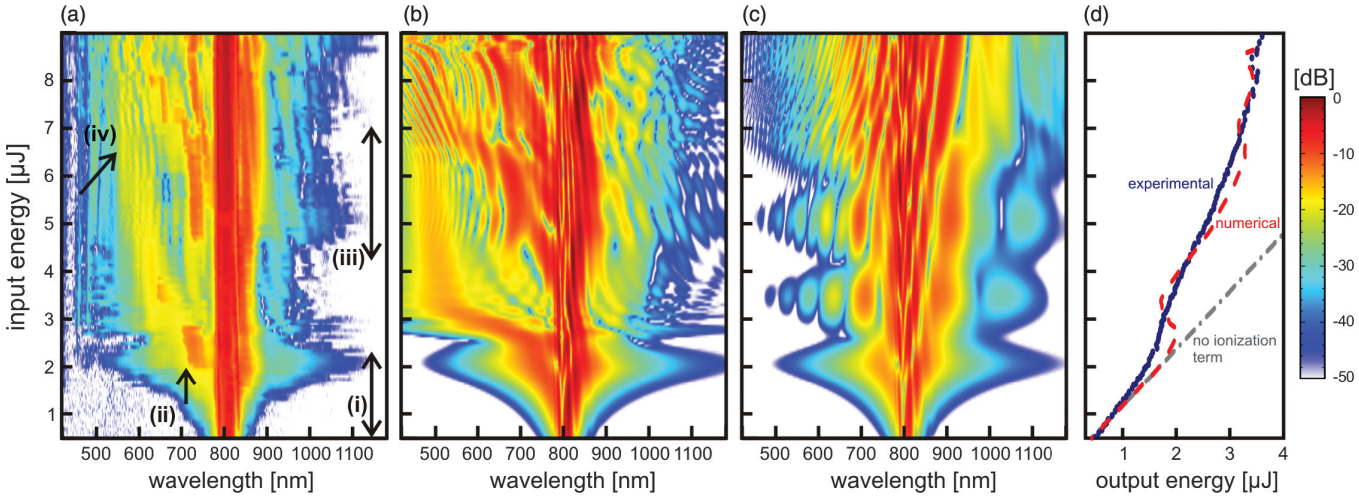

FIG. 2 (color). (a) Experimental and (b) numerical output spectra of a kagome PCF (26 μm diameter) filled with 1.7 bar of argon as a function of input pulse energy. For comparison, (c) shows numerical modeling without the ionization term. In region (i) there is no ionization, at (ii) a blue shoulder emerges, moving to higher frequencies as the pulse energy increases; at (iii) a second ionization stage starts; and at (iv) spectral interference between the two blueshifting pulses is apparent. Output energies as a function of input energies are shown in (d). Both modeling (red dashed line) and the experiment (blue dotted line) show deviations from a linear increase in transmission at points coinciding with the emission of the blueshifted pulses. In the absence of ionization, propagation is affected only by linear fiber losses (gray dash-dotted line).

Pulse propagation in this system was numerically modeled by incorporating an ionization term, based on quasistatic tunneling [16], in the unidirectional nonlinear optical field equation [17–19], including the radial dependence of the ionization rate. This term describes the generation of free electrons at high optical field intensities and the backaction on the pulse through plasma-based phase modulation and ionization-related losses. The phase and amplitude profiles of the pump pulses were carefully measured with frequency-resolved optical gating and used in the simulations, which also included the experimentally measured loss spectrum of the fiber.

Numerical simulations [shown in Fig. 2(b)] including the ionization term confirm the experimental observations (both spectral evolution and transmission losses), whereas the agreement is very poor when it is omitted [Fig. 2(c)]. This indicates that the frequency up-conversion process reported here is distinctly different from self-scattering mechanisms that depend either on the Raman effect [20,21] or on the presence of a zero-dispersion point close to the pump wavelength [22,23]. There are some small discrepancies between the simulations and experiment, for example, the extent of the blueshift. These are likely due to the particular choice of the ionization model or the neglect of polarization. Figure 2(d) shows good agreement between experimentally and numerically determined energy losses when we include ionization.

In the absence of ionization, the pulses will self-compress to a minimum duration related to the soliton order. The presence of an ionization threshold has the effect of arresting this compression process before it reaches completion. When a sufficiently energetic pulse is compressed in the gas-filled fiber [Fig. 3(a)], it ionizes the atoms, causing a field-dependent lowering of the refractive index which does not recover within the duration of the pulse [Fig. 3(b)], i.e., imposing a positive phase shift [Fig. 3(a)] and a consequential shift to higher frequencies [24–26]. This corresponds to the emission of a blueshifted spectral band. Thereafter, the residual pump pulse, if its energy is sufficiently high, will experience a further cycle of compression and ionization, followed by emission of a second blueshifted pulse.

Figure 4(a) shows numerical simulations of the evolution of the temporal envelope of an 8 μJ pulse (soliton number $N \sim 10$) as it propagates along the fiber. After $\sim$15 cm, the pulse has compressed to a few-cycle pulse with a peak intensity of $\sim 2 \times 10^{14}$ W/cm^2. After this point, the peak intensities remain much higher than at the input, oscillating up and down with distance as the cycles of compression come and go. Figure 4(b) shows that a blue-spectral shoulder emerges at the compression point, reaching out by more than 250 nm, i.e., 174 THz. Additional blueshifted pulses are generated at successive recompression points at $\sim$20 and $\sim$25 cm. Figure 4(c) shows calculated cross-correlation frequency-resolved optical gating spectrograms at selected distances. These show that the blue-spectral sidebands emerge as individual solitons, walking off from the pump pulse during propagation. Note that continuous blueshifting upon further propagation in this system in a manner opposite to the Raman self-frequency redshift is addressed in a separate theoretical study [9].

A unique feature of ionization in a fiber optical context is that the pulse and plasma can interact over extended length scales without the constraints of maintaining self-guidance, as required in filamentation. The competing effects of transient plasma formation and Kerr nonlinearity are given by [27]

$$\Delta n = n_2 I - \omega_p^2/(2 n_0 \omega_o^2), \tag{1}$$

where n_2 is the nonlinear refractive index and I the intensity. The second term takes account of the presence of the plasma where n_0 is the linear refractive index, ω_0 the pump frequency, and ω_p the plasma frequency: $\omega_p = [N_e e^2/(m_e \varepsilon_o)]^{0.5}$, where N_e is the free-electron

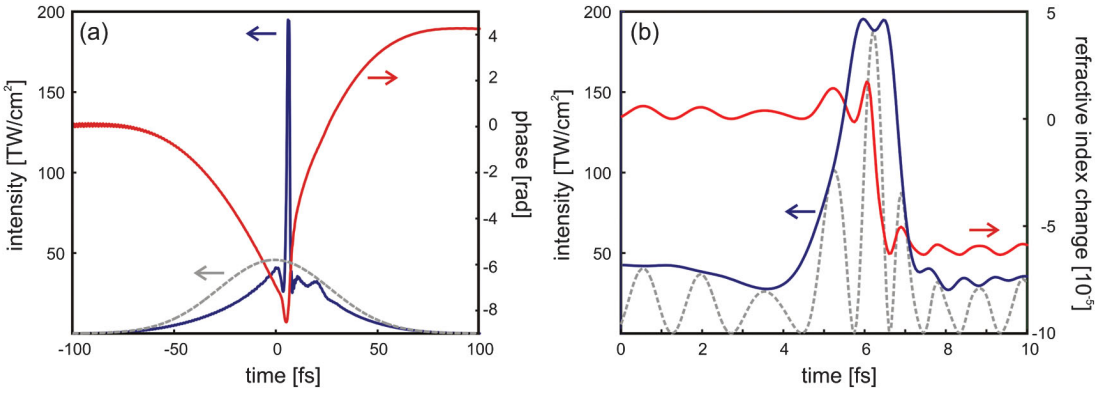

FIG. 3 (color). Numerical calculations for an 8 μJ pulse at maximum compression: (a) intensity envelope (blue line) and temporal phase (red line); a net positive phase shift can be seen. For comparison, the envelope of the launch pulse is also shown (gray dashed line). (b) Close-up of the same pulse: intensity envelope (blue line), oscillatory field (gray line), and refractive index change (red line); for high field strength, the index drops due to free-electron generation.

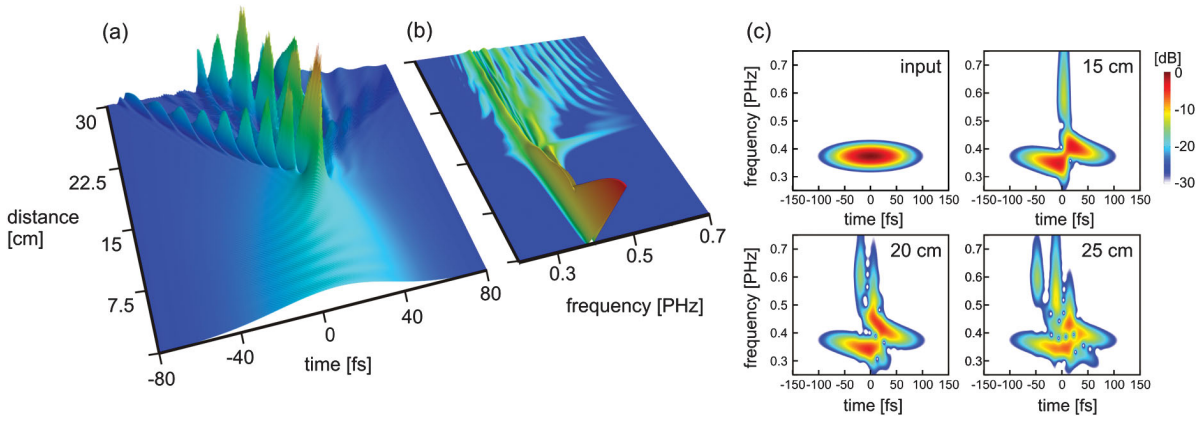

FIG. 4 (color). Temporal evolution of an 8 μJ pulse [(a) linear scale]: The peak power is increased by a factor of ~4 at a distance of 14 cm. Even after the pulse breakup, the peak power remains on a level higher than the input pulse and can lead to subsequent ionization stages. Corresponding spectral evolution [(b) linear scale]: Temporal compression leads to the ejection of a blueshifted pulse at frequencies of 550 THz. [(c) Log scale]: Numerical time-frequency snapshots (cross-correlation frequency-resolved optical gating spectrograms) at characteristic distances for a 65 fs, 8 μJ pump pulse using a 10 fs gate function. The ejection of blueshifted pulses is shown for frequencies around 0.6 PHz.

density, ε_0 the vacuum permittivity, e the electronic charge, and m_e the electron mass. The two terms in Eq. (1) are plotted in Fig. 5 against propagation distance. After 10 cm, plasma effects appear, reaching ionizing fractions of 0.5% at a distance of ~14 cm. At this position, the total nonlinear refractive index change is negative and 3 times greater in magnitude than the highest Kerr index change. Beyond this point, the residual pulse energy is high enough to cause several further ionization events over ~10 cm until it falls to a value too low for significant further ionization.

In conclusion, gas-filled kagome hollow core PCF makes it possible to study soliton-plasma interactions in a single-mode guiding system with well-controlled and adjustable dispersion. Self-compression of higher-order solitons down to durations of a few optical cycles results in the ejection of one or more blueshifted pulses due to the creation of a plasma at high intensities (~ 10^{14} W/cm^2). The system is ideal for detailed studies of intense light-matter interactions, i.e., extended propagation in ionized media [9], or exploring the possibility of Kerr effect saturation at high intensities [28]. It will also be useful for high harmonic generation driven directly by self-compressed oscillator pulses operating at high repetition rates [29]. Additionally, the inclusion of a process that depends on the instantaneous electric field invites a closer look at carrier envelope effects [2]. The ability to operate in entirely new parameter regimes seems likely to transform the field of light-plasma interactions, as well as creating new possibilities in nonlinear fiber optics.

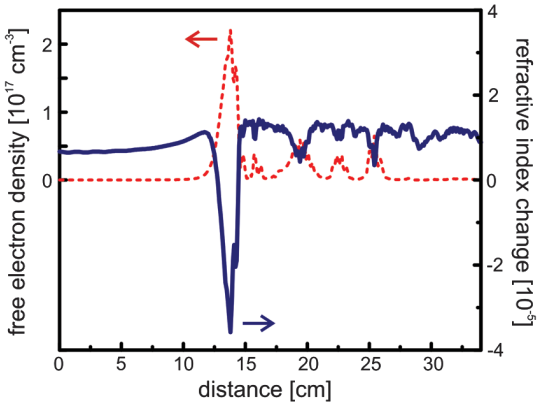

FIG. 5 (color). Numerically calculated free-electron density (left axis) and total (Kerr plus plasma) nonlinear refractive index change (right axis) as a function of propagation distance for an 8 μJ pulse. The maximum free-electron density is 2.2×10^{17} cm^{-3} (ionization fraction of 0.5%), resulting in a refractive index change of -3.4×10^{-5}. Ionization can be maintained over 10 cm through the fiber.

[1] P. B. Corkum, Phys. Rev. Lett. **71**, 1994 (1993).
[2] T. Brabec and F. Krausz, Rev. Mod. Phys. **72**, 545 (2000).
[3] T. Popmintchev, M.-C. Chen, P. Arpin, M. M. Murnane, and H. C. Kapteyn, Nat. Photon. **4**, 822 (2010).
[4] L. F. Mollenauer, R. H. Stolen, and J. P. Gordon, Phys. Rev. Lett. **45**, 1095 (1980).
[5] J. K. Ranka, R. S. Windeler, and A. J. Stentz, Opt. Lett. **25**, 25 (2000).
[6] P. St. J. Russell, J. Lightwave Technol. **24**, 4729 (2006).
[7] N. Y. Joly, J. Nold, W. Chang, P. Hölzer, A. Nazarkin, G. K. L. Wong, F. Biancalana, and P. St. J. Russell, Phys. Rev. Lett. **106**, 203901 (2011).
[8] P. K. A. Wai, H. H. Chen, and Y. C. Lee, Phys. Rev. A **41**, 426 (1990).

[9] M. F. Saleh, W. Chang, P. Hölzer, A. Nazarkin, J. C. Travers, N. Y. Joly, P. St. J. Russell, and F. Biancalana, following Letter, Phys. Rev. Lett. **107**, 203902 (2011).
[10] G. P. Agrawal, *Nonlinear Fiber Optics* (Academic, New York, 2006), 4th ed.
[11] L. Bergé, S. Skupin, R. Nuter, J. Kasparian, and J.-P. Wolf, Rep. Prog. Phys. **70**, 1633 (2007).
[12] M. Nisoli, S. Stagira, S. De Silvestri, O. Svelto, S. Sartania, Z. Cheng, M. Lenzner, C. Spielmann, and F. Krausz, Appl. Phys. B **65**, 189 (1997).
[13] O. H. Heckl, C. R. E. Baer, C. Kränkel, S. V. Marchese, F. Schapper, M. Holler, T. Südmeyer, J. S. Robinson, J. W. G. Tisch, F. Couny, P. Light, F. Benabid, and U. Keller, Appl. Phys. B **97**, 369 (2009).
[14] A. B. Fedotov, E. E. Serebryannikov, and A. M. Zheltikov, Phys. Rev. A **76**, 053811 (2007).
[15] J. Nold, P. Hölzer, N. Y. Joly, G. K. L. Wong, A. Nazarkin, A. Podlipensky, M. Scharrer, and P. St. J. Russell, Opt. Lett. **35**, 2922 (2010).
[16] M. V. Ammosov, N. B. Delone, and V. P. Krainov, Sov. Phys. JETP **64**, 1191 (1986).
[17] P. Kinsler, Phys. Rev. A **81**, 013819 (2010).
[18] M. Geissler, G. Tempea, A. Scrinzi, M. Schnürer, F. Krausz, and T. Brabec, Phys. Rev. Lett. **83**, 2930 (1999).
[19] W. Chang, A. Nazarkin, J. C. Travers, J. Nold, P. Hölzer, N. Y. Joly, and P. St. J. Russell, Opt. Express **19**, 21018 (2011).
[20] E. M. Dianov, A. Ya. Karasik, P. V. Mamyshev, A. M. Prokhorov, V. N. Serkin, M. F. Stel'makh, and A. A. Formichev, JETP Lett. **41**, 294 (1985).
[21] F. M. Mitschke and L. F. Mollenauer, Opt. Lett. **11**, 659 (1986).
[22] V. N. Serkin and V. A. Vysloukh, in *Nonlinear Guided Wave Phenomena*, Technical Digest Vol. 14 (Optical Society of America, Washington, DC, 1993), p. 236.
[23] S. P. Stark, A. Podlipensky, and P. St. J. Russell, Phys. Rev. Lett. **106**, 083903 (2011).
[24] N. Bloembergen, Opt. Commun. **8**, 285 (1973).
[25] W. M. Wood, C. W. Siders, and M. C. Downer, IEEE Trans. Plasma Sci. **21**, 20 (1993).
[26] S. P. Le Blanc, R. Sauerbrey, S. C. Rae, and K. Burnett, J. Opt. Soc. Am. B **10**, 1801 (1993).
[27] P. Sprangle, J. R. Peñano, and B. Hafizi, Phys. Rev. E **66**, 046418 (2002).
[28] P. Béjot, J. Kasparian, S. Henin, V. Loriot, T. Vieillard, E. Hertz, O. Faucher, B. Lavorel, and J.-P. Wolf, Phys. Rev. Lett. **104**, 103903 (2010).
[29] T. Südmeyer, S. V. Marchese, S. Hashimoto, C. R. E. Baer, G. Gingras, B. Witzel, and U. Keller, Nat. Photon. **2**, 599 (2008).